

# Research Journal of Pharmaceutical, Biological and Chemical Sciences

## Analysis of Manufacturing Features of MEMS Thermoelectrical IR Detectors.

**Yuri Anatolievich Krupnov\***, Gennady Ivanovich Oreshkin, Dmitry Borisovich Rygalin, and Alexander Victorovich Larchikov.

National Research University of Electronic Technology (MIET), Shokina Sq., Build. 1, Zelenograd, Moscow, 124498, Russia.

### ABSTRACT

The paper presents a theoretical study of the influence of parameters of technological layers of thermoelectrical detectors of infrared radiation on the accuracy of temperature measurements of thermal objects. The results demonstrate that for thermocouples from polycrystalline silicon noise equivalent temperature difference for 64x64 matrix can reach 10 mK for cases of operation with frame refresh rate of 10 Hz. It was established that the specific resistance of thermocouples, which minimizes noise equivalent temperature difference, is equal to  $4.5 \cdot 10^{-5} \Omega \cdot \text{cm}$ . It was demonstrated that the increase of number of thermocouples connected serially in an element leads to the increase of noise equivalent temperature difference, and the increase is proportional to square root from the number of elements. The study contains the investigation into the relationship between noise equivalent temperature difference and design parameters of devices: area of cell, thickness, length and width of polycrystalline silicon of thermocouples, and thickness of silicon dioxide of a membrane. The study introduces a term "maximum frame refresh rate" and defines its influence on noise equivalent temperature difference.

**Keywords:** IR-Radiation, Noise Equivalent Temperature Difference, Frame Refresh Rate, Seebeck Coefficient, Polycrystalline Silicon, Thermocouple, Membrane.

*\*Corresponding author*

## INTRODUCTION

Infrared detectors in the long-wave infrared part of spectrum (8-14  $\mu\text{m}$ ) are divided into photon detectors and thermal detectors [10]. Photon detectors are based on the measurement of the number of electrons or holes, which are generated by incident radiation. Thermal detectors measure the change of temperature caused by absorbed radiation through different mechanisms, including the change of electrical resistance, polarizability, thermoelectricity and thermal expansion [10], [16], [3], [8]. In spite of the fact that photon detectors have higher sensitivity, thermal detectors are more suitable for systems with low cost, because photon detectors, generally, require cooling to cryogenic temperatures [10], [11].

Nowadays non-cooled matrix detectors of IR-radiation based on microbolometers are the most widely spread type of devices [4], [13], [14], [17], [15]. Matrices belonging to that type with format up to 640x480 and discriminable temperature difference up to 50 mK are developed and already produced.

Recently, despite of the evident advances in the development of non-cooled matrix detectors of IR-radiation based on microbolometers, the interest for detectors based on thermoelectrical detectors is increasing. Thermocouple matrices have competitive cost, as compared to other engineering solutions used in thermography and non-contact measurement of temperature, such as thermal imaging microbolometers, in which it is required to obtain image of environment and, at the same time, high spatial resolution is not necessary: for example, face detection, survey of critical temperature of a surface, detection of hot points and surveillance cameras. Other applications can be found in the field of process control in manufacturing industry, air condition control, detection of passengers with fever, fire detection and warning. Advantages of that technology are lower cost, low energy consumption, short response time, as well as higher sensitivity and detection capability of the sensor.

Despite of the large numbers of published studies on thermoelectrical matrix detectors of IR-radiation, so far there are no studies, which focus on detailed analysis of design features of manufacturing of detectors microthermocouples. The presented paper is an attempt to fill that gap.

### Calculation of the main characteristics

The design of a MEMS detector (detector of microelectromechanical system) of thermal radiation based on thermocouples, consists of one or several serially connected semiconductor thermocouples, which are placed on a thin membrane and have a common characteristic structure: "cold" junction is located on heat sink, which is, generally, is silicon substrate, and "hot" junction is located on the thin membrane. If absorber located on the membrane is affected by infrared radiation from a heated object, flux of radiation between the film and the object will heat the membrane. As a result, the thermocouple will produce voltage due to Seebeck effect. Generally, during design the dominating process of thermal transfer from "hot" (absorbing part of the membrane) to "cold" contacts (the substrate) is thermal conductivity of the membrane and the thermocouples, which are situated on them. For the reason that thermal flux value is defined by Fourier law [12], it is obvious that creation of bigger temperature gradient between "hot" and "cold" contacts requires decrease of cross-section area of the membrane's traverses and/or increase of their length. At that, other ("parasite") heat flows, which are decreasing temperature gradient, should be excluded. Firstly, it concerns thermal conductivity of gas atmosphere, which surrounds the membrane. Thus, elimination of that thermal losses due to vacuumization allows to increase sensitivity for, approximately, 20 times with larger areas of the membrane (more than  $100 \times 100 \mu\text{m}^2$ ) [6].

The most important operational characteristics of IR-radiation detectors are accuracy of temperature detection of thermal objects and frame refresh rate. Noise Equivalent Temperature Difference (NETD) is the characteristic of accuracy of temperature detection of thermal objects by a photodetector.

For a thermocouple the output electrical signal is determined by the change of the temperature of a detector and the thermal EMF of junction; the main source of noise of thermocouples is, generally, the thermal noise (Johnson noise) of its ohmic resistance.  $1/f$  noise, which is the crucial parameter of microbolometers, is not necessary to consider in that case, because currents are not passing through a thermocouple in the measurement mode the open-circuit voltage. At the same time, the measurement mode the open-circuit voltage, is the main mode for thermal thermocouple detectors.

The main channel of losses of heat, received by a photodetector element in a vacuumized detector, is its evacuation through elements of the thermocouple and the console of the membrane. In principle, heat evacuation through consoles of the membrane is a "parasite" effect, which is unrelated to the process of receiving a response to input effect. Therefore, it is desirable to eliminate it by selection of materials of the membrane consoles in a way, which makes thermal conductivity of consoles much lower than total thermal conductivity of thermocouples. In that case the increase of the membrane temperature, and, therefore, temperatures of "hot" junction of the thermocouples located on it ( $\Delta T$ ), and caused by decrease of strength of incident IR-radiation ( $\Delta P$ ) are related by the following expression:

$$\Delta T = \frac{\Delta P}{G}, \quad (1)$$

and the open-circuit voltage:

$$\Delta V = \alpha \cdot \Delta T = \frac{\alpha \cdot \Delta P}{G}, \quad (2)$$

where  $\alpha$  – total thermal EMF of both legs of the thermocouple,  $G$  – total thermal conductivity of the thermocouple, which is calculated as  $G = G_1 + G_2$ , where  $G_1$  and  $G_2$  – thermal conductivities of the thermocouple's elements.

Current passing through the thermocouple in the same direction, in which current is passing in the case of heating the detector, causes cooling of the heated seam due to Peltier effect, which leads to appearance of EMF in the opposite direction. As a result, the equivalent electrical layout of the thermocouple can be presented in the form demonstrated in Figure 1. In Figure 1  $R$  is the ohmic resistance of the circuit,  $R_d$  is the dynamic resistance caused by Peltier effect and equal to:

$$R_d = \frac{\alpha^2 T}{G}, \quad (3)$$

$C_e$  – effective capacitance of the circuit, which is calculated using the equation:

$$C_e = \frac{C}{\alpha^2 T}, \quad (4)$$

where  $C$  – thermal capacity of the the photodetector element.

Considering that the power current generator can be calculated using the equation:

$$I = \frac{\Delta P}{\alpha T}, \quad (5)$$

the open-circuit voltage is as follows (the same as in (2)):

$$\Delta V = I \cdot R_d = \frac{\alpha \cdot \Delta P}{G}, \quad (6)$$

and time constant in the open-circuit mode is calculated using the equation:

$$\tau = C_e \cdot R_d = \frac{C}{G}, \quad (7)$$

Dynamic resistance of the thermocouple  $R_d$  can be identified by means of regular electrical measurements. For instance, by means of DC bridge the sum of  $R + R_d$  can be measured, and by means of AC bridge  $R$  is measured; the measurements should be carried out at low currents, in order to make heating due to Joule heating effect negligible.

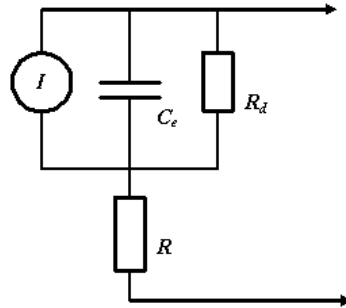


Fig. 1. Equivalent layout of the thermocouple

Johnson noise of the thermocouple is calculated as follows:

$$\overline{(\Delta V_f^2)} = 4k_B T R_t B, \tag{8}$$

where  $k_B$  – Boltzmann constant,  $R_t$  – effective resistance of the thermocouple,  $B$  – width of frequency band of electronic system for signal registration. Noises, which occur as the results of spontaneous fluctuations of the detector's temperature, are expressed through the Johnson law of dynamic resistance  $R_d$ ; thus, the total noise voltage can be expressed by the following equation:

$$\overline{(\Delta V^2)} = 4k_B T (R + R_d) B, \tag{9}$$

Maximum efficiency of thermoelectrical transformation is achieved, when parameters of sections of the thermocouple are selected in a way that the product of its total thermal conductivity  $G$  and total electrical resistance  $R$  is minimal [19]:  $G \cdot R = \min$ . This condition is met if the following conditions are satisfied:

$$\frac{l_1 \cdot S_2}{l_2 \cdot S_1} = \sqrt{\frac{k_1 \cdot \rho_2}{k_2 \cdot \rho_1}}, \tag{10}$$

where  $k_1, k_2$  and  $\rho_1, \rho_2$  are, respectively, specific thermal conductivity and effective specific resistance of sections 1, 2 of the thermocouple;  $l_1, l_2$  and  $S_1, S_2$  are, respectively, their length and cross-section area.

In that case total electrical resistance of the thermocouple  $R$  can be expressed as follows:

$$R = \frac{\lambda T}{G}, \lambda = (\sqrt{\lambda_1} + \sqrt{\lambda_2})^2, \tag{11}$$

where  $\lambda_1 = \frac{G_1 R_1}{T}$ ,  $\lambda_2 = \frac{G_2 R_2}{T}$  – Lorentz numbers,  $T$  – absolute temperature,  $G_{1,2} = k_{1,2} \cdot S_{1,2} / l_{1,2}$ ,  $R_{1,2} = \rho_{1,2} \cdot l_{1,2} / S_{1,2}$  – respectively, thermal conductivity and electrical resistance of sections 1 and 2 of the thermocouple,  $G = G_1 + G_2$ ,  $R = R_1 + R_2$ . Therefore, for the case of the simple thermocouple with similar sections:

$$\lambda = (\sqrt{k_1 \rho_1} + \sqrt{k_2 \rho_2})^2 / T.$$

Sensitivity of the image detector for increase of the temperature of a radiation source  $\Delta T_e$  as compared to background is calculated as follows:

$$S_{TT} = \Delta T / \Delta T_e, \tag{12}$$

It is evaluated in comparison with absolute black body, which has universal radiation capability. Assuming, that  $\Delta T_e$  is minor and taking into account (1), the following expression is obtained:

$$S_{TT} = A \frac{\eta q_j}{G_t}, \tag{13}$$

where  $A$  – area of the photodetector element,  $\eta$  – absorbing capability of the element,  $q$  – parameter, which characterizes focusing optical system and geometry of sensitive element in the plane of the image (in case of placement of a sensor element near a focal plane of an optical system with transparency of  $t_0$ , input diaphragm diameter  $D$  and equivalent focal distance  $F$ ,  $q \approx D^2 t_0 / 4F^2$ ). In the above we considered that  $\Delta P = \eta q j \cdot A$ , where  $j \approx 2.563 \text{ W/m}^2 \cdot \text{K}$  for band of IR-radiation  $8 \div 14 \mu\text{m}$ .

Volt sensitivity of thermoelectric sensor to change of temperature of irradiating body  $\Delta T_e$  is, according to (2) and (12), equal to:

$$S_v = \Delta V / \Delta T_e = \alpha \cdot S_{TT} = \frac{\alpha \eta q j}{G_t} \cdot A \quad (14)$$

For highly sensitive elements with minimum thermal conductivity of elements of the thermocouple it is necessary to consider also radiation losses  $G_r$ , which occur due to radiation by surface of the photodetector element:

$$G_r = 4A\sigma T^3, \quad (15)$$

where  $\sigma = 5.670373(21) \times 10^{-8} \text{ W} \cdot \text{m}^{-2} \cdot \text{K}^{-4}$  – Stefan-Boltzmann constant. Therefore, the total heat emission in that case will be defined by effective thermal conductivity:

$$G_t = G + G_r. \quad (16)$$

Then, using the equations (2), (3), (9), (10), (13) and (14), we can obtain the equation of distribution of NETD:

$$NETD = \frac{\sqrt{(\Delta V^2)}}{S_v} = \frac{\sqrt{4k_B T^2 (\lambda/a^2 + 1) G_t B}}{A \eta q j} \quad (17)$$

The equation (17) defines the limit of accuracy of measurement of thermal objects' temperature by the photodetector of image with signal to noise ratio of  $S/N = 1$ . The right part of the equation (17) depends on the used materials and design parameters of the element. The required limit of accuracy of measurement of thermal objects' temperature  $\Delta T_{min}$  of the developed detector on the design stage can be achieved by solving the multiparameter problem:

$$\frac{\sqrt{4k_B T^2 (\lambda/a^2 + 1) G_t B}}{A \eta q j} < \Delta T_{min} \quad (18)$$

The equations (17, 18) are not convenient for use in practice, therefore, we reformulated (17) in more convenient form, which clarifies the relationship between NETD and design parameters: At that, we assume that the detector is vacuumized and the thermal losses of the sensitive element are defined only by thermal conductivity of the thermocouples. As the material of the thermocouples we selected polycrystalline silicon of n-type and p-type, which allows to implement standard CMOS technology. The expression (18) contains width of transmission frequency band of the electronic signal registration system.

Let's define frequency bands, which are defined by electronic equipment for registration and processing. In order to calculate a matrix with  $m \times n$  size ( $m$  – number of strings,  $n$  – number of columns) with parallel reading of string for the time of frame  $f_k^{-1}$ , necessary frequency of strings, which is equal to  $f_{str} = m f_k$ . The length of a string is divided by time, which is necessary for reading of the signal of string at output, and time, which is necessary for the fixation of an input signal, which is defined by the integrator, i.e.  $t_{str} = t_{read} + t_{int}$ . As it known, frequency band of the integrator is  $1/2t_{int}$ . Let's assume that  $t_{read} = t_{int}$ , then  $B = t_{int}/2 = 2m f_k = 2m f_{kmax} (f_k / f_{kmax})$ , thus, obtaining:

$$NETD = 2\pi c_M t_M (f_{kmax})^{3/2} \{4k_B T N_T \rho_T (l_T / w_T) m f_k / f_{kmax}\}^{1/2} (\alpha_T N_T \eta q j)^{-1} \quad (19)$$

where  $c_m$  – specific thermal capacity of the membrane;  $w, t, l$  – dimensions of the thermocouple (membrane): width, thickness and length;  $N_T$  – number of thermocouples in a cell, placed on the membrane;  $m$  – number of strings in matrix;  $f_{kmax}$  – maximum frame refresh rate, which was identified from the analysis of the dynamic mode.

In the dynamic mode photoresponse of the thermocouple is described by the equation:

$$\Delta V = \frac{\alpha \Delta T}{\sqrt{1+(\omega\tau)^2}} = \frac{\alpha \Delta P}{G_t \sqrt{1+(\omega\tau)^2}}, \quad (20)$$

where  $\tau$  – time constant (7),  $\omega=2\pi f$ ,  $f$  – frame refresh rate. In that case volt sensitivity of the photodetector is equal:

$$S_v(f) = \frac{\alpha \eta q j A}{G_t \sqrt{1+(2\pi f \tau)^2}}. \quad (21)$$

From the given equation it can be concluded that maximum frame refresh rate can be defined from the condition  $2\pi f_{kmax} \tau = 1$ . Then, considering that thermal losses of the sensitive element are defined by thermal conductivity of thermocouples:

$$f_{kmax} = \frac{1}{\pi} (\kappa_T w_T t_T / l_T) N_T (c_M A t_M)^{-1}, \quad (22)$$

where  $\kappa_T$  – specific thermal conductivity of the thermocouple's section.

Thus, the expressions (19) and (22) provide a theoretical basis for the analysis of relationship of limiting parameters of a thermoelectric detector and its design parameters. It is worth mentioning, that those expressions are derived with the assumption that thermal losses of the membrane are completely defined by thermal conductivity of thermocouples [2], and the dominating noise is the thermal noise (Johnson noise).

Design parameters of the detector must be selected and coordinated in the way that value of NETD will be minimum and, therefore, minimum limit of accuracy of measurement of temperature distribution of an object  $\Delta T_{min}$  is achieved in that case. During analysis we will consider constants of technological layers from the Table 1.

**Table 1. Values of thermal characteristics**

Parameters	Si*	Si <sub>3</sub> N <sub>4</sub>	SiO <sub>2</sub>	Au	nichrome
$c_s, J/m^3 \cdot K$	$1.7 \cdot 10^6$	$1.8 \cdot 10^6$	$1.9 \cdot 10^6$	$2.5 \cdot 10^6$	$3.78 \cdot 10^6$
$\kappa_s, W/m \cdot K$	20-30	15-20	1 (0.9)		11.3

In addition, we assume that console of the membrane, on which "hot" junction of the thermocouples is located, is layer of SiO<sub>2</sub>, because implementation of a membrane produced from silicon nitride increases thermal conductivity of traverses with thermocouples more than in two times. That fact, in turn, increases the maximum frame refresh rate ( $f_{kmax}$ ) (see (22)), and, therefore, increases the value of NETD, which is proportional to  $(f_{kmax})^{3/2}$  (see (19)). Thus, in order to achieve the maximum temperature resolution, it is necessary, as much as possible, to exclude thermal conductivity console of the membrane, which must be considered as a "parasite" process.

From the analysis of the equation (19), first of all, it is clear that the increase of number of thermocouples on the membrane doesn't lead to the desired outcome, i.e. the decrease of value of NETD, despite of the fact that the transformation coefficient of thermocouples is increasing proportionally to their number. Indeed, by inserting (22) in (19) we obtain that the value of NETD with other conditions equal is increasing proportionally to the square root of the number of thermocouples, i.e.  $NETD \sim N_T^{-1/2}$ . At that, the equation (14) allows to conclude that the value of output signal from a thermoelectric detector in that case doesn't depend on number of thermocouples. The increase of the number of thermocouples leads to the decrease of NETD proportionally to  $N_T^{-1/2}$  only in case if thermal losses in a detector are defined by the thermal

conductivity of the membrane's console. However, the value of NETD itself in that case becomes bigger than for  $G_T > G_M$  ( $G = G_T + G_M$ ).

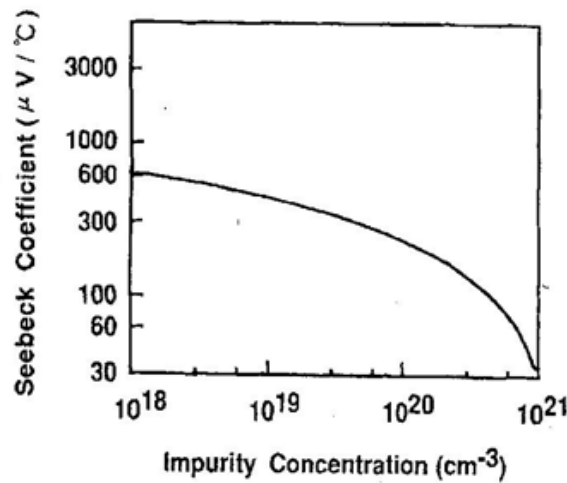


Fig. 2. Relationship between Seebeck coefficient for polycrystalline silicon and concentration of doping impurity [10]

Thermoelectrical matrix detectors of IR radiation, which are produced nowadays, contain several tens of thermocouples and have thermal resolution of order of 0.2-0.5 K; only devices, which are announced for production in the near future, are designed with one or two thermocouples per cell [6].

The second parameter, the value of which significantly influences NETD, is the value of specific resistance of polycrystalline silicon. Two members of the equation (19) depend on the specific resistance of polycrystalline silicon: the value of thermal noise (Johnson noise) of the thermocouple and the value of Seebeck coefficient. Figure 2 [10] presents the experimental relationship between Seebeck coefficient for polycrystalline silicon and concentration of doping impurity in the desired range of doping concentrations, and Figure 3 [20] shows the relationship between specific resistance of the polycrystalline silicon and degree of doping.

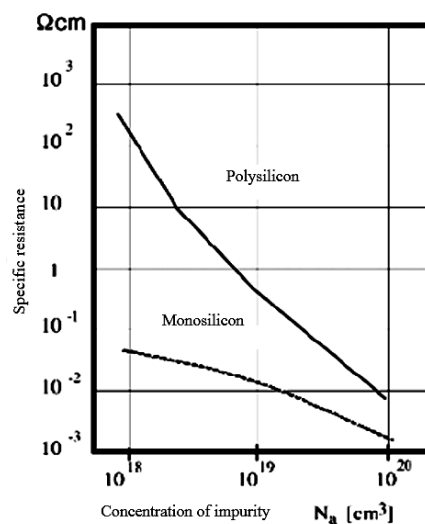


Fig.3. Relationship between specific resistance of polycrystalline silicon and concentration of doping impurity [20]

Figure 2 shows that in a case of low concentration of the impurity, i.e. for low specific resistance of polycrystalline silicon, Seebeck coefficient becomes almost independent from degree of doping; at the same time, thermal noise of the thermocouple seriously increases, which causes the increase of NETD (see 19)). In the opposite case, i.e. big concentration of a doping impurity, Seebeck coefficient value seriously decreases, which also results in the increase of NETD. Thus, the relationship between NETD and specific resistance of the

thermocouple must have a minimum value. In order to find that minimum value, we differentiated the expression for NETD (19) by  $\rho_T$  and by equating the derivative to zero found specific resistance of the thermocouple, which provide minimum value of NETD. Using generally accepted relationship between Seebeck coefficient and electric conductivity of the thermocouple  $\alpha_T \sim \ln(\rho_T/\rho_0)$  [1], [7], we obtain the following expression:  $\rho_T(\text{NETD} = \text{NETD}_{\min}) \approx 7.45\rho_0$ . The value of  $\rho_0$  is obtained on the basis of the experimental data (Figure 2, 3) by means of approximation of the experimental curve by minimization of standard deviation [9]. Thus, the found specific resistance  $\rho_0$  is equal to  $6.05 \cdot 10^{-5} \Omega \cdot \text{cm}$ , and the relationship between Seebeck coefficient and specific resistance is approximated by the equation:

$$\alpha_T = 41.4 \cdot \ln(\rho_T/\rho_0) \tag{23}$$

Chart of function  $F(\rho_T) = (\rho_T/\rho_0)^{1/2} / \ln(\rho_T/\rho_0)$  is presented in Figure 4.

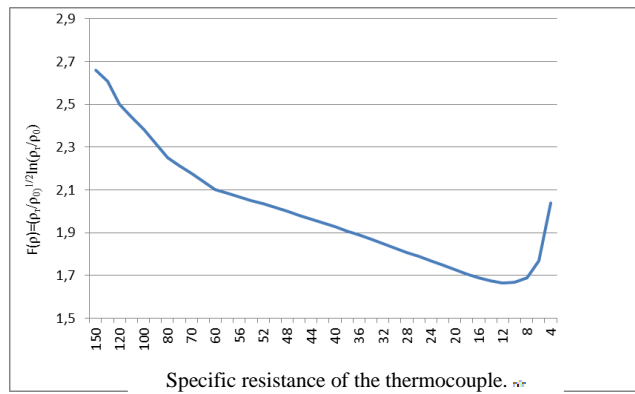


Fig. 4. Relationship between the function  $F(\rho_T) = (\rho_T/\rho_0)^{1/2} / \ln(\rho_T/\rho_0)$  and specific resistance of the thermocouple's polycrystalline silicon

As it can be seen from Figure 4, in the range of specific resistance  $\rho_T = (8 \div 70)\rho_0$  and the concentration of the doping impurity from  $8 \cdot 10^{19}$  to  $6 \cdot 10^{20} \text{ cm}^{-3}$  the value of NETD doesn't seriously change with the change of specific resistance, approximately 30%, and rapidly increases only with the further increase of specific resistance NETD. That defines the optimal range of doping of polycrystalline silicon of the thermocouple. The value of specific resistance, which minimizes the value of NETD, is  $\rho_T = 7.45\rho_0 \approx 4.5 \cdot 10^{-4} \Omega \cdot \text{cm}$ , Seebeck coefficient in that case is  $\approx 83.3 \mu\text{V/K}$ .



Fig. 5. Relationship between NETD and maximum frame refresh rate with consideration of optimization of doping of a polycrystalline silicon of the thermocouple (membrane  $\text{SiO}_2$ ,  $t_m = 0.2 \mu\text{m}$ ,  $t_r = 0.2 \mu\text{m}$ ,  $l_r/w_r = 25$ ,  $N_r = 1$ ,  $\chi_r = 30 \text{ V/m} \cdot \text{K}$ ,  $c_m = 1.9 \cdot 10^6 \text{ J/m}^3 \cdot \text{K}$ ,  $\rho_r = 12 \Omega/\text{sq}$ ,  $\alpha_r = 84 \mu\text{V/K}$ , matrix  $64 \times 64$ )

The third parameter, which significantly influences the value of NETD, is the maximum frame refresh rate ( $f_{kmax}$ , see (19)). The relationship between NETD from maximum frame refresh rate is presented in Figure 5.

Generally, for television systems frame refresh rate is specified as one of the system's parameters. Two modes of operation of that system are possible: full-frame mode with frame refresh rate of 50-60 Hz and low-frame mode with frame refresh rate of, approximately, 10 Hz. Leaving aside the possibility of realization of those frame refresh rates in a real device, it can be seen from (19) that in order to achieve limiting thermal resolution of a detection of IR radiation it is necessary to design a cell with the lowest possible maximum frame refresh rate. In other words, it is desirable to have a maximum frame refresh rate, which is equal to the system's frame refresh rate. Maximum frame refresh rate is described by the equation (22).

As it can be seen, the expression (22) includes physical constants of the used layers: specific thermal conductivity of the thermocouple and specific thermal capacity of the membrane, as well as geometry parameters of layers of polycrystalline silicon of the thermocouple and thickness of the membrane. Thickness of layers are defined by technological capabilities and can't change in wide range. The only value, which can change in a wide range, is a cell's area. For the reason that the length of the thermocouple is, approximately, equal to the linear dimension of a cell's side, it can be assumed that  $l_T \approx (A)^{1/2}$ . Then, approximate estimating expression for maximum frame refresh rate:

$$f_{kmax} = \frac{1}{\pi} \cdot (\kappa_T w_T) N_T / (c_M A^{3/2}). \tag{24}$$

Relationship between maximum frame refresh rate and sizes of the cell is presented in Figure 6.

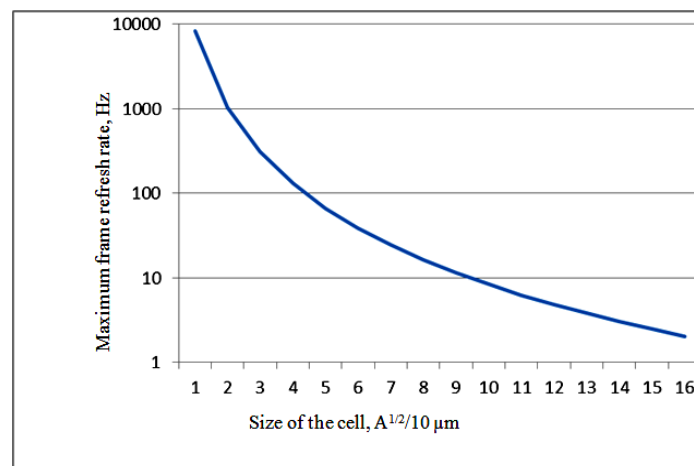
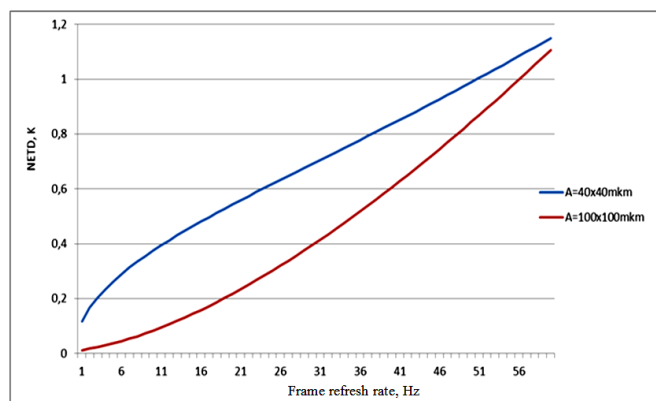


Fig. 6. Relationship between maximum frame refresh rate and sizes of the cell (membrane  $SiO_2$ ,  $t_m = 0.2 \mu m$ ,  $t_r = 0.2 \mu m$ ,  $l_r/w_r = 25$ ,  $N_r = 1$ ,  $\kappa_r = 30 \text{ V/m}\cdot\text{K}$ ,  $c_m = 1.9 \cdot 10^6 \text{ J/m}^3 \cdot \text{K}$ ,  $\rho_r = 12 \Omega/\text{sq}$ ,  $\alpha_r = 84 \mu\text{V/K}$ , matrix  $64 \times 64$ )

The analysis of the relationship between NETD and parameters of the cell and technological layers implied that the system's frame refresh rate is equal to maximum frame refresh rate. However, in fact frame refresh rate in the system may be both bigger or smaller than the maximum frame refresh rate, at that, the difference can be significant. From the expression (19) it can be concluded that if the maximum frame refresh rate is bigger than the system's frame refresh rate, then NETD is decreasing proportionally to square root from the equation  $f_k/f_{kmax}$ . In the opposite case, when the maximum frame refresh rate is smaller than the system's frame refresh rate, then NETD value is increasing with the frame refresh rate. In the limit case, when  $f_k \gg f_{kmax}$ , NETD value is increasing proportionally to  $(fk)^{3/2}$ . Relationship between NETD from the system's frame refresh rate is presented in Figure 5.



**Fig.7. Relationship between NETD and the system's frame refresh rate (membrane  $\text{SiO}_2$ ,  $t_m = 0.2 \mu\text{m}$ ,  $t_r = 0.2 \mu\text{m}$ ,  $l_r/w_r = 25$ ,  $N_r = 1$ ,  $\kappa_r = 30 \text{ V/m}\cdot\text{K}$ ,  $c_m = 1.9 \cdot 10^6 \text{ J/m}^3 \cdot \text{K}$ ,  $\rho_r = 12 \Omega/\text{sq}$ ,  $\alpha_r = 84 \mu\text{V/K}$ , matrix  $64 \times 64$ )**

From Figure 7 it can be concluded that for low-frame systems ( $f_k=10 \text{ Hz}$ ) the value of NETD for a matrix of  $64 \times 64$  elements can be less than  $20 \text{ mK}$  for the size of an element of  $100 \times 100 \mu\text{m}^2$ , which is comparable with the best detectors of IR radiation based on microbolometers, with an exception of the matrix's size [11].

The carried out analysis establishes a basis for evaluation of prospectiveness of any design of a cell based on thermocouples produced using MEMS technology. For example, the study of Toshio et al. [18] describes the thermal matrix detector of IR radiation based on MEMS thermoelectrical detector produced from polycrystalline silicon with  $100 \times 100 \mu\text{m}^2$  cell size. At that, the area of the membrane, which is sensitive to IR radiation, is  $80 \times 84 \mu\text{m}^2$ . The thickness of the membrane made from silicon dioxide is  $0.450 \mu\text{m}$ . 32 "hot" junctions of thermocouples from polycrystalline silicon of n-type and p-type are situated at each cell of the membrane. The thickness of polycrystalline silicon is  $0.07 \mu\text{m}$ , and its width is  $0.6 \mu\text{m}$ . The concentration of the doping impurity of polycrystalline silicon, in average, is  $5 \cdot 10^{19} \text{ cm}^{-3}$ , and Seebeck coefficient is  $350 \mu\text{V/K}$ . The average length of a microthermocouple is  $30 \mu\text{m}$ . Thermocouples are serially connected by aluminum buses in order to reduce resistance of thermopile. The average length of a microthermocouple's section is  $35 \mu\text{m}$ . The experimental measurements of NETD produced the result of  $0.5 \text{ K}$  for the frame refresh rate of  $30 \text{ Hz}$ . From the description above it can be seen that the parameters of a cell's layers are far from optimum. A simple decrease of the number of thermocouples from 32 to 1 decreases NETD in 5 times. Moreover, as it can be seen from the Figures 2, 3, 4, the increase of the concentration of the impurity in polycrystalline silicon to  $2 \cdot 10^{20} \text{ cm}^{-3}$  leads to the additional decrease of NETD in 3 times. Thus, even such simple optimization makes it possible to achieve NETD values in the range of  $30\text{-}40 \text{ mK}$ .

## CONCLUSION

The presented example shows the importance of the obtained results for optimization of cells' design: parameters of technological layers and number of thermocouples.

In addition, there is the fact that, as it can be seen from Figure 7, the decrease of the size of a cell to  $40 \times 40 \mu\text{m}$  leads to the rapid increase of NETD. First of all, it is related with sufficiently low sensitivity of thermocouples produced from polycrystalline silicon, which Seebeck coefficient at optimum specific resistance is only about  $83 \cdot 10^{-6} \text{ V/K}$ . From that perspective, implementation of microthermocouples produced from other pair of materials, for example, n-silicon – p-silicon, can significantly decrease NETD. Indeed, for the case of polycrystalline silicon, as well as for monocrystalline silicon relationship between Seebeck coefficient and specific electrical conductivity is of the same nature  $\alpha_r = \alpha_{r0} \ln(\rho_r/\rho_0)$  [5]. However,  $\alpha_{r0}$  for polycrystalline silicon is equal to  $41.4 \mu\text{V/K}$ , i.e. 5 times bigger. Moreover,  $\rho_0$  for monocrystalline silicon is bigger by order  $\rho_0 = 5 \cdot 10^{-4} \Omega \cdot \text{cm}$ . All of those leads to advantage in value of NETD for more than 15 times (see (19)).

The presented paper is based on the results of the applied research carried out on the basis of Contract No. 14.578.21.0059 between MIET and the Ministry of Education and Science of the Russian Federation. Unique identification number of applied research works – RFMEFI57814X0059.

## REFERENCES

- [1] Budzier, H. and G. Gerlach, 2011. Thermal Infrared Sensors. Wiley.
- [2] Cho, D., S. Kumar and W. Carr, 1991. Electrostatic Levitation Control System for Micromechanical Devices. Patent US5015906.
- [3] Choi, I.H. and K.D. Wise, 1986. A Silicon-Thermopile-Based Infrared Sensing Array for Use in Automated Manufacturing. IEEE Trans. Electron Devices, 1(33): 72-79.
- [4] FLIR, n.d.. FLIR A65/A35/A15/A5. Date Views 02.09.2015 [www.flir.ru/automation/display/?id=56341](http://www.flir.ru/automation/display/?id=56341).
- [5] Foote, M.C., M. Kenyon, T.R. Krueger et al., 2004. Thermopile Detector Arrays for Space Science Applications. Proceedings of SPIE, 2474: 98-109.
- [6] Forg, B., F. Herrmann et al., 2014. Thermopile Sensor Array with Improved Spatial Resolution, Sensitivity and Image Quality. Photonics, 1: 98-103.
- [7] Herwaarden, A.W. and P.M. Sarro, 1986. Thermal Sensors Based on the Seebeck Effect. Sensors and Actuators, 10: 321-346.
- [8] Kenny, T.W., J.K. Reynolds, J.A. Podosek, E.C. Vote, L.M. Miller, H.K. Rockstad and W.J. Kaiser, 1996. Micromachined Infrared Sensors Using Tunneling Displacement Transducers. Rev. Sci. Instrum., 1(67): 112-128.
- [9] Kirsanov, K.B., 2009. Organization of Processing and Storage of Data Tails Coming from Sensors in Parallel Program Systems. Information, Measurement and Control Systems, 6(7): 69-71.
- [10] Kruse, P.W. and D.D. Skatrud, 1997. Uncooled Infrared Imaging Arrays and Systems. Academic Press.
- [11] Kruse, P.W., 1995. A Comparison of the Limits to the Performance of Thermal and Photon Detector Imaging Arrays. Infrared Phys. Technol., 5(36): 869-882.
- [12] Landau, L. and A. Lifschitz, 1985. Theoretical Physics (Vol. 8). Moscow: Science.
- [13] Livejournal, 2014, January 8. Thermographic Camera for Smartphone, 2014. Date Views 03.09.2015 [russ-79.livejournal.com/49519.html](http://russ-79.livejournal.com/49519.html).
- [14] LLC Infratest, n.d. Thermographic Modules. Date Views 06.09.2015 [www.thermoframe.ru/index.html](http://www.thermoframe.ru/index.html).
- [15] LLC SPC Spektr-AT, n.d. Thermographic Module "Thermal-Eye 3600AS Series". Date Views 12.09.2014 [www.spektr-at.ru/catalogue/teplo/TE3600AS.html](http://www.spektr-at.ru/catalogue/teplo/TE3600AS.html).
- [16] Muralt, P., 2001. Micromachined Infrared Detectors Based on Pyroelectric Thin Films. Rep. Prog. Phys., 10(64): 1339-1388.
- [17] Specialized Information System "Equipment for Special Services", n.d.. IR-module "Thermal-Eye 4500AS" L-3 COMMUNICATIONS (USA). Date Views 12.09.2015 [www.sis-tss.ru/2010-06-23-20-11-19/3709-ik-modul-thermal-eye-4500as-l-3-communications.html](http://www.sis-tss.ru/2010-06-23-20-11-19/3709-ik-modul-thermal-eye-4500as-l-3-communications.html).
- [18] Toshio, K. et al., 1994. Uncooled Infrared Focal Plane Array Having 128 × 128 Thermopile Detector Elements. In Proc. SPIE 2269, Infrared Technology XX, 450, pp: 450-459.
- [19] Wilson, M.L., D. Kubisiak, R.A. Wood, J.A. Ridley and M. Listvan, 1991. An Uncooled Thermo-Electric Microthermopile Camera Developed Using Silicon Microstructure Sensors. In Proc. IRIS Spec. Group Infrared Detect., Boulder, CO.
- [20] Zee, S., 1981. Physics of Semiconductor Devices. Moscow: Mir.